

We are IntechOpen, the world's leading publisher of Open Access books Built by scientists, for scientists

6,900

Open access books available

186,000

International authors and editors

200M

Downloads

Our authors are among the

154

Countries delivered to

TOP 1%

most cited scientists

12.2%

Contributors from top 500 universities



WEB OF SCIENCE™

Selection of our books indexed in the Book Citation Index
in Web of Science™ Core Collection (BKCI)

Interested in publishing with us?
Contact book.department@intechopen.com

Numbers displayed above are based on latest data collected.
For more information visit www.intechopen.com



Topology Optimization Method Considering Cleaning Procedure and Ease of Manufacturing

Takeo Ishikawa

Additional information is available at the end of the chapter

<http://dx.doi.org/10.5772/63153>

Abstract

This chapter proposes a novel topology optimization method for the material distribution of electrical machines using the genetic algorithm (GA) combined with the cluster of material and the cleaning procedure. Moreover, the obtained rotor structure was assumed to consist of the simple shape of PMs in order to consider ease of manufacturing. The rotor structure of a permanent magnet (PM) synchronous motor is designed and manufactured. The optimized rotor has 32% more average torque than that of the experimental motor with the same stator. The effectiveness of the proposed method is verified.

Keywords: topology optimization, genetic algorithm, permanent magnet synchronous motor, finite element method, manufacturing

1. Introduction

There are several design techniques to optimize electrical machines and electromagnetic devices. However, most of these techniques were restricted to the optimization of a couple of parameters defining the shape. I think that the first step of optimal design should design the topology of these structures by starting from an empty space. Topology optimization allows obtaining an initial conceptual structure starting with minimal information regarding the structure of the object. Topology optimization methods are very promising and, therefore, were proposed about 20 years ago [1, 2]. Since then, several papers have been published in this field. For example, reference [3] proposed a topology optimization using design sensitivity. Reference [4] proposed an ON/OFF sensitivity method and hybridized it with the GA in order to improve convergence characteristics. Reference [5] designed an electromagnetic

system by a topology optimization method considering magnetization direction. Reference [6] proposed a topology optimization method coupling with magneto-thermal systems. Reference [7] designed a 3D electromagnetic machine with soft magnetic composite core. Reference [8] proposed a topology optimization method using the GA and ON/OFF sensitivity in conjunction with a blurring technique in order to avoid small structure spots. Reference [9] took into account a mapping function to improve convexity in the topology optimization procedure. Reference [10] applied a topology optimization method to a coupled magnetic structural problem. Reference [11] designed an IPM motor using the ON/OFF method. Reference [12] optimized magnetic actuators by a level-set method. Reference [13] optimized an inductor by the evolutionary algorithm. Reference [14] proposed a 3D topological optimization method based on the multistep utilization of GA. Reference [15] presented a possible solution to the structural optimization problem using a simple heuristic search algorithm.

The author proposed a topology optimization method to optimize the distribution of materials within an electrical machine using the GA [16]. In addition, he proposed a concept for the cluster of materials and a cleaning procedure for the materials and designed the stator of a brushless DC motor based on this method [17]. However, that study considered only two types of materials, air, and iron, and therefore, it is similar to the ON/OFF method. He improved the previous method in order to consider more than two materials namely, air and iron as well as r -oriented, x -oriented, and y -oriented magnets [18]. Moreover, initially, the obtained rotor structure was assumed to consist of the simple shape of PMs in order to consider ease of manufacturing [19].

This chapter summarizes the novel topology optimization method for the material distribution of electrical machines using the GA combined with the cluster of material and the cleaning procedure. Moreover, the obtained rotor structure was assumed to consist of the simple shape of PMs in order to consider ease of manufacturing. The proposed method is applied to the design of the rotor structure of PM synchronous motor. It is an interior permanent magnet synchronous motor (IPMSM) used for air-conditioning. The average torque characteristics of IPMSMs are compared with the commercialized motor.

2. Proposed topology optimization method

In this section, the topology optimization method is briefly explained, which is implemented in this study. GA is an algorithm that imitates the evolution of living things and is suitable for problems with a large sample space. In the proposed method, the design region is split into finite element meshes, and the materials of several elements—for example, a cell—are associated with a gene in the chromosome. For example, if we consider three types of materials—for example, air, iron, and magnet, which are set to 0, 1, and 2, respectively—the chromosome is composed of some genes as shown in **Figure 1**. Two parents are selected randomly, and some genes are selected to be exchanged by a uniform crossover with a crossover ratio, and then, two new children are generated as shown in **Figure 1**. The chil-

dren inherit the good characteristics of parents by repeating the process. We proposed the concept of the cluster with many types of materials. For example, irons 2 and 3 form the same cluster because they are next to each other as shown in **Figure 2a**, and iron 4 forms another cluster. If the area of cluster is narrow, that is, the number of cells in the same cluster is smaller than or equal to an integer N_{min} , a cleaning procedure is introduced. When N_{min} is equal to 2, irons 2 and 3 remain, iron 1 is changed to the surrounding material air, and iron 4 is changed to the magnet. As a result, this cleaning method has the ability of removing floating pieces of the material.

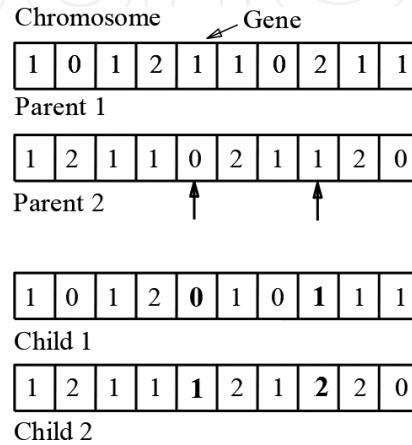


Figure 1. Example of genes and uniform crossover in GA.

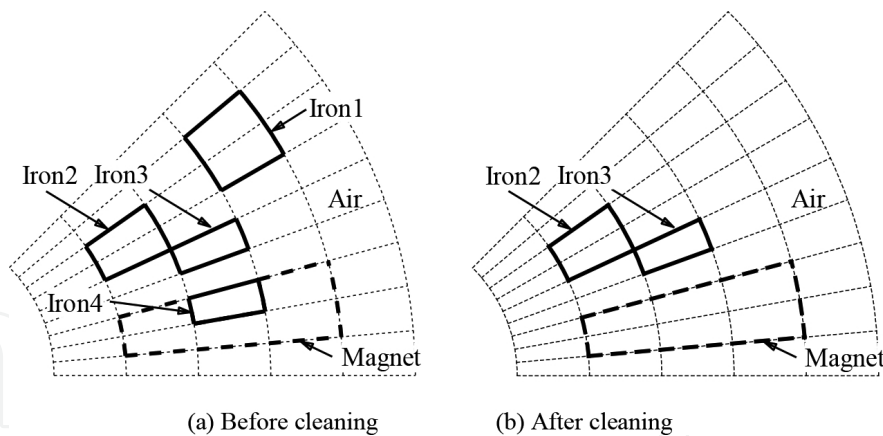


Figure 2. Cluster of materials and the cleaning method concept.

Figure 3 shows the cross section of a four-pole PM synchronous motor with distributed windings. One-eighth of the rotor is designed for symmetry. This study iterates the GA with the newly increased length of genes. For the first iteration, a coarse topology is designed using a small number of design variables in a 5×9 array of cells as shown in **Figure 4a**. Three magnetized directions of permanent magnet are dealt with as shown in **Figure 5**. **Figure 6** shows the treatment of the cluster of material on the boundary. The y -oriented magnet has the same magnetized direction; on the contrary, the x - and r -oriented magnets have the opposite

direction at both sides of periodic boundary. Therefore, the numbers of cells in the cluster of air, iron, and y -oriented magnet are doubled. On the other hand, the numbers of cells in the cluster of air, iron, and r -oriented magnet are doubled at both sides of symmetric boundary, because the r -oriented magnet has the same magnetized direction.

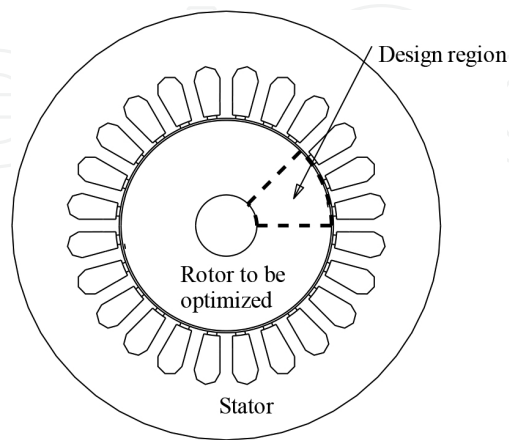


Figure 3. Motor cross section and design region.

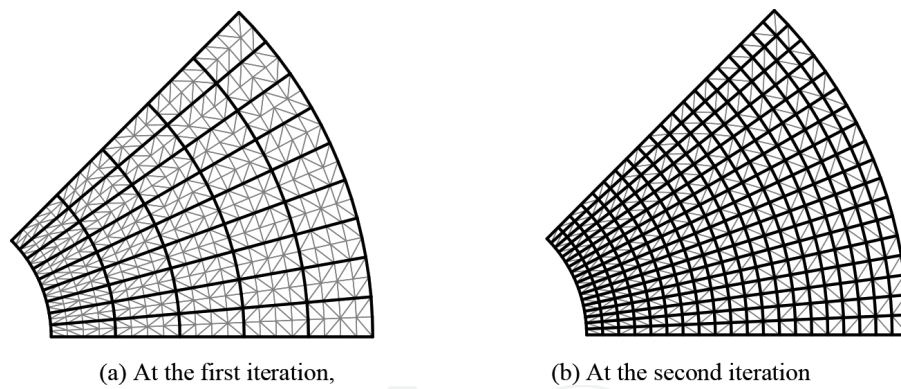


Figure 4. Cell at each iteration.

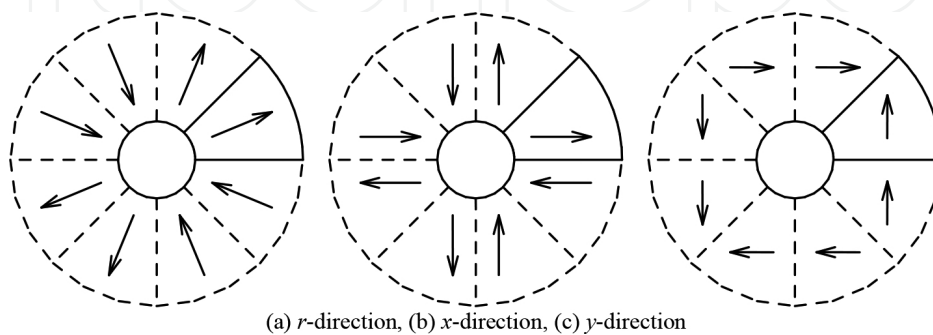


Figure 5. Magnetized direction in permanent magnets.

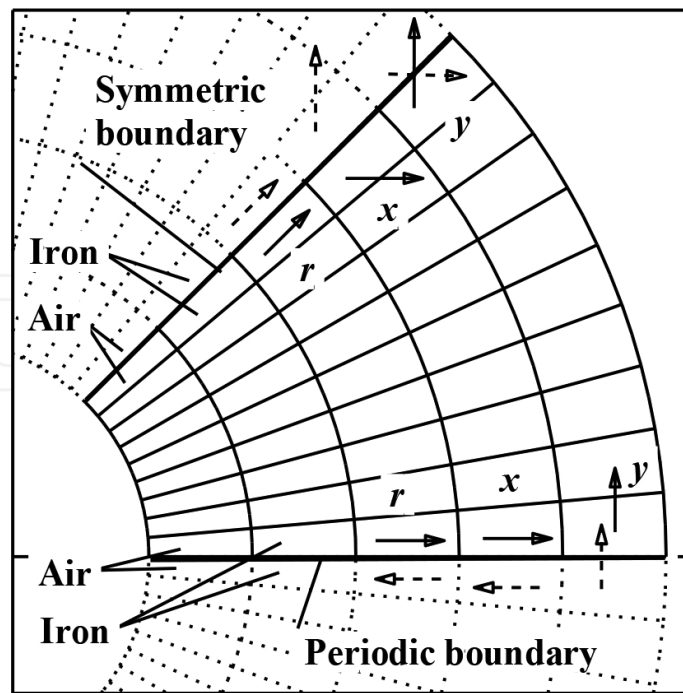


Figure 6. Cluster of material on the symmetric boundary and on the periodic boundary.

A fine topology then is designed using a large number of design variables for the second iteration in a 20×18 array of cells as shown in **Figure 4b**. For the second iteration, a set of initial individuals in the GA inherit the individual that has the best fitness at the conclusion of the previous iteration. For example, the initial material in cell P_0 is generated by a probability of $1/5$ from materials in cells $P_0, P_1, P_2, P_3,$ and P_4 shown in **Figure 7**. The whole flow-chart for the proposed method is shown in **Figure 8**. The parts highlighted by the thick line are newly added to the conventional GA with the elite selection. The parameter N_{min} of the cleaning procedure at each iteration is listed in **Table 1**.

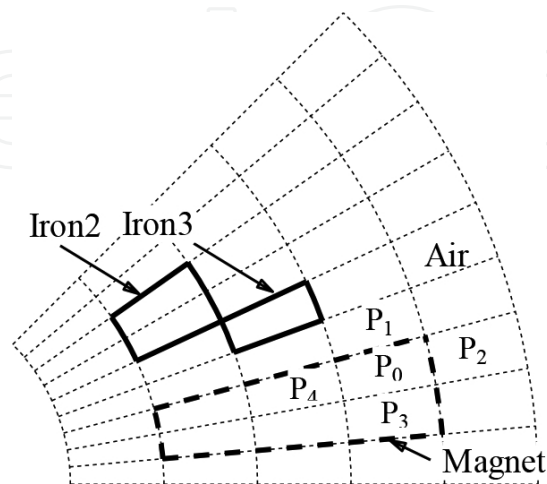


Figure 7. Cluster of material on the symmetric boundary and on the periodic boundary.

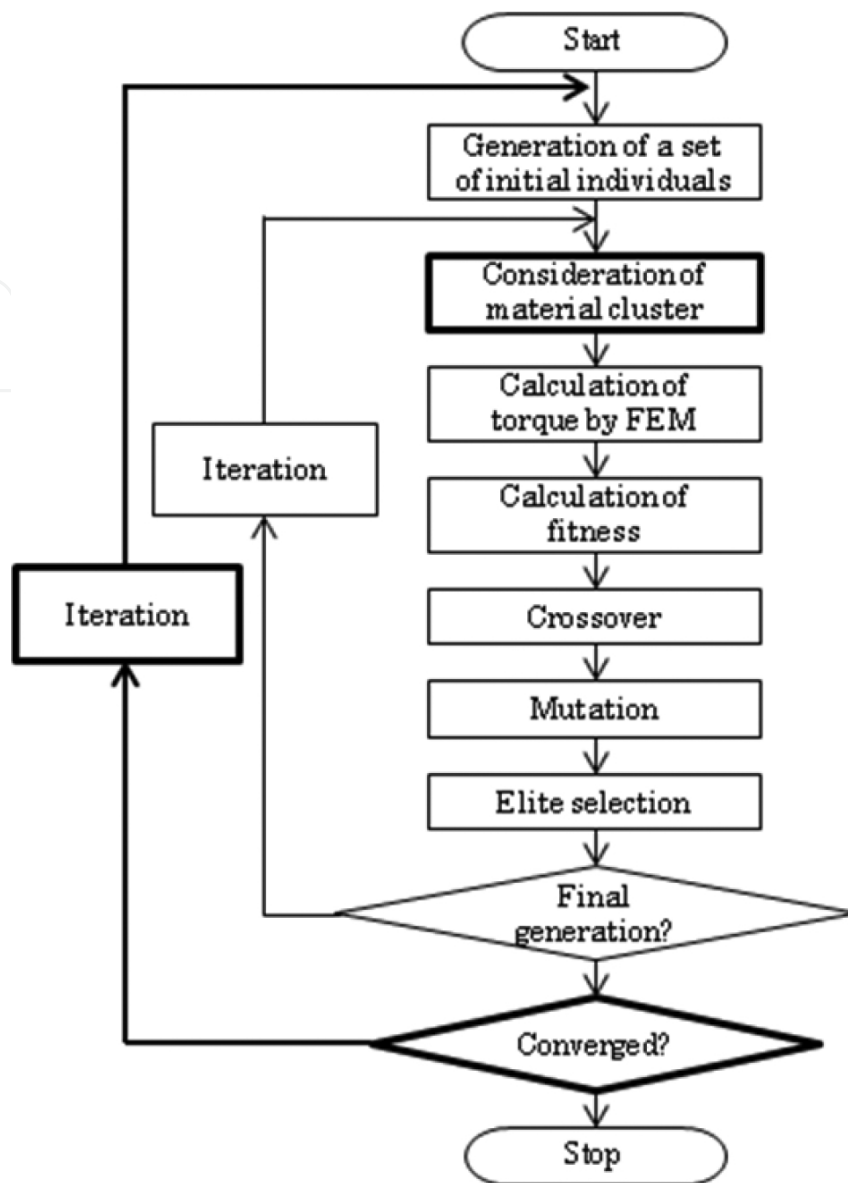


Figure 8. Flowchart for the proposed topology optimization method.

| Figures | Material | N_{min} at first iteration | N_{min} at second iteration |
|------------|------------------------------------|------------------------------|-------------------------------|
| Figure 10a | Air, iron, r -oriented PM | 1 | 4 |
| Figure 10b | Air, iron, x -, y -oriented PM | 1 | 4 |
| Figure 10c | Air, iron, x -, y -oriented PM | 1 for air and iron, 0 for PM | 4 |
| Figure 10d | Air, iron, r -oriented PM | 0 | 0 |

Table 1. Design parameters.

3. Rotor structure obtained by the topology optimization method

We optimize the topology of the rotor structure by considering two types of PMs; r -oriented magnet only and both x - and y -oriented magnets. The number of populations is set to 45. If a number larger than 45 is selected, there is a possibility for a better result. However, this would lead to a longer computational time. **Figure 9** shows a convergence characteristic of the applied topology optimization. We find that the fitness functions almost converge at every iteration, namely at every 300th generation.

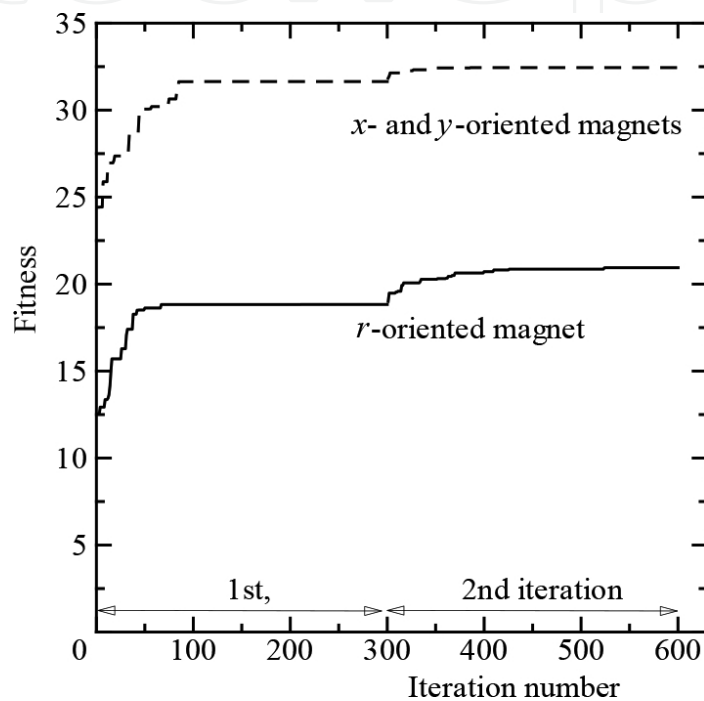


Figure 9. Convergence characteristic of the topology optimization.

Figure 10a shows the obtained rotor structure, in which three types of materials—air, iron, and the r -oriented magnet—are taken into account. N_{min} at the first iteration is equal to 1. This means that if the number of cells in the cluster is <2 , the material of the cluster is changed to the material of surrounding cells. At the second iteration, N_{min} is chosen to 4. Design parameters are shown in **Table 1**. The optimization by considering the r -oriented magnet only produces a kind of surface PM-type rotor. **Figure 10b, c** shows the obtained rotor structure by considering x - and y -oriented magnets that produce a kind of interior PM-type rotor. The parameters listed in **Table 1** are used for the cleaning procedure. The rotor shapes appear as V and W . The V shape was obtained when the cleaning procedure was carried out for the PM material at the first iteration, and the W shape was obtained when the cleaning procedure was not carried out for the PM material at the first iteration. **Figure 10d** shows the obtained rotor structure when the cluster of material and the cleaning method are not carried out. T_{ave} and V_{pm} for **Figure 10d** are 5.38 Nm and 23.2 cm³, respectively, and for **Figure 10a**, they are 6.16 Nm and 31.6 cm³, respectively. Although the obtained

magnet shape appears similar to that shown in **Figure 10a**, the rotor has numerous small pieces of iron in the r -oriented magnet. As mentioned above, the cleaning procedure can remove the small cluster of materials. Therefore, the structure obtained without considering the cleaning procedure has numerous small pieces of iron in the magnet and numerous pockets of air in the iron, which are shown in **Figure 10d**. This rotor has a complicated weak structure and is difficult to manufacture.

The optimized rotor shapes shown in **Figure 10b, c** appear as V and W . Let us discuss what causes this difference. **Figure 11** shows the obtained shapes at the first iteration with and without considering the cleaning procedure for the PM materials. When the cleaning procedure is not carried out for PM materials, small PM cells can easily remain in the GA procedure. As a result, **Figure 11a** does not include the x -oriented magnet at the center, whereas **Figure 11b** includes the x -oriented magnet at the center. The x -oriented magnet shown in **Figure 11b** remains in the next iteration, and the final shape, which includes the x -oriented magnet, is then obtained as shown in **Figure 10c**.

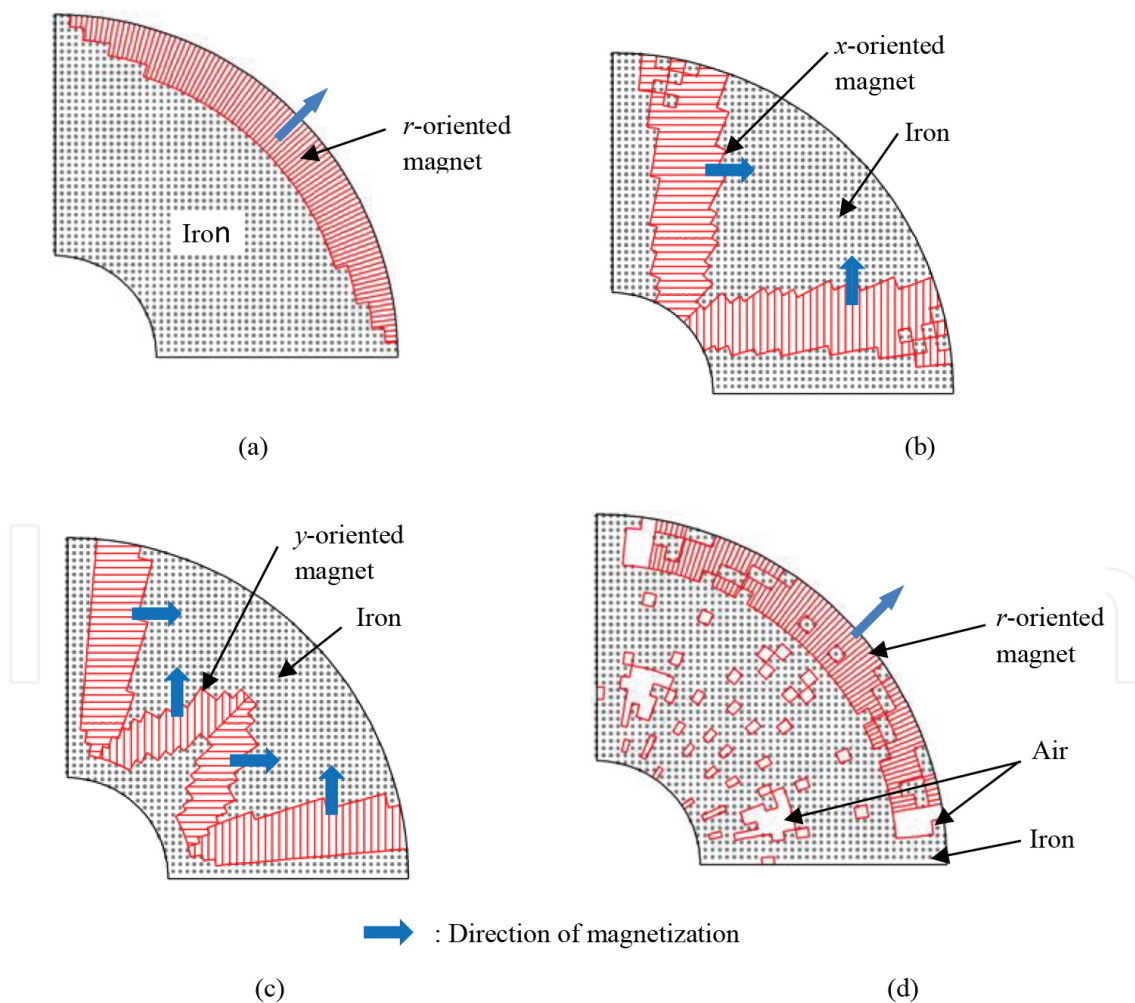


Figure 10. Rotor structure obtained by the proposed topology optimization with the parameter shown in **Table 1**.

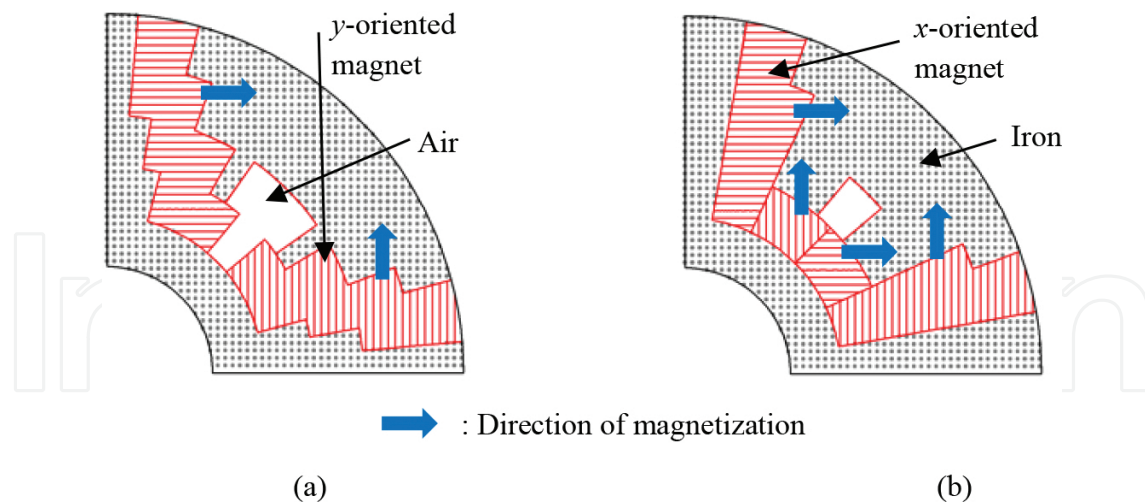


Figure 11. Rotor structures obtained at the first iteration by considering air, iron, x - and y -oriented PMs, (a) with and (b) without the cleaning procedure for the PM.

4. Optimization considering ease of manufacturing

The obtained rotor structures are complex and impractical. In order to consider the ease of manufacturing, magnets and air pockets are assumed to be simple shapes, and they are then optimized using conventional techniques. For example, the rotor structures shown in **Figure 12a** can be assumed to be similar to the ones in **Figure 10a**, where the magnets are represented by four parameters. The rotor structure shown in **Figure 10b, c** can be assumed to contain four hexahedron PMs as shown in **Figure 12b**. In this shape, the rotor structure is represented by six parameters if the thickness of the magnets is uniform and the volume of the magnets is specified. We assume that the shape of each magnet is a hexahedron and the magnet is magnetized in the vertical direction as shown in **Figure 12b** for the ease of magnetization. Moreover, we assume that a core area is introduced on the surface of the rotor as shown in **Figure 12b** to insure machine strength against centrifugal force. Therefore, parameter r_3 is fixed, and then, the number of design parameters becomes five.

An example to be optimized is the rotor of an experimental motor. This experimental motor is well known as the D model in IEE Japan for an air-conditioner and has an IPM-type rotor. A full-search method to optimize the rotor shape is used, because we want to verify that there is a good rotor shape similar to those shown in **Figure 10b, c**. The angle of position A is set to five values, and the radius and angle of position B and C , respectively, are also set to five values. This gives $5^5 = 3125$ patterns to be calculated in the full-search method. This study iterates the full-search method twice, where the variation of each parameter is set to approximately half, and the phase angle of stator current is set to 15° , 20° , 25° , and 30° . The finite element mesh is generated automatically using the Delaunay method, and the torque is calculated using the Maxwell's tensor method in the full-search method.

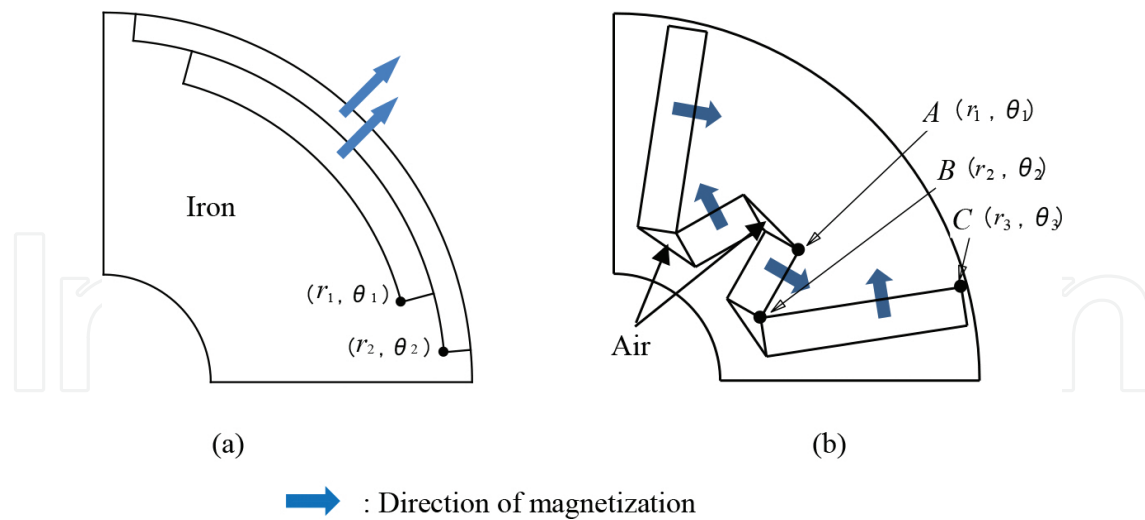


Figure 12. Rotor structures represented by simple magnet shape.

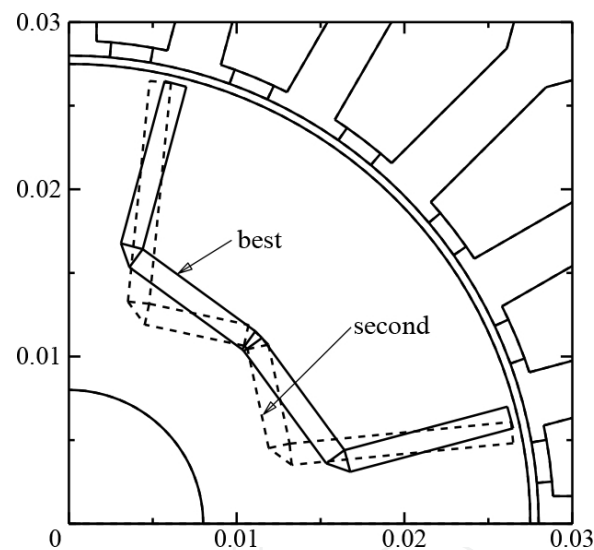


Figure 13. Obtained rotor structure of the air-conditioner.

Figure 13 shows the obtained rotor structure, where the “best” rotor structure provides the largest average torque at the second iteration of the full-search method, and the “second” one provides the second-largest average torque at the first iteration. It was found that the “best” rotor structure is *U*-shaped and the “second” is *W*-shaped. Figure 14a shows the obtained rotor structure and its flux distribution at no load. Figure 14b shows the flux distribution of the experimental motor whose stator is the same as that shown in Figure 14a. The ratings of the experimental motor are 3000 min^{-1} , 1.5 kW , 192 V , and 5.6 A , and the stator outer diameter, the rotor diameter, and the air-gap length are 112 , 55 , and 0.5 mm , respectively. Figure 14 shows that the flux lines of the optimized motor are increased by approximately 50%, because the magnets are wider and thinner than the experimental motor. It is found from Figure 15 that the average torque is increased from 5.8 to 7.6 Nm —that is, by approximately 32%—

mainly due to the increase of magnetic flux linkage. However, the torque ripple of the proposed motor is increased because it is not considered by the fitness function. The calculated torque of the “second” rotor structure is almost the same as that of the “best” rotor structure. This means that the shape of the PM in the inside rotor is not a significant factor in the torque provided. Therefore, we believe that two types of rotor structure have been obtained by the proposed method as shown in **Figure 10b, c**.

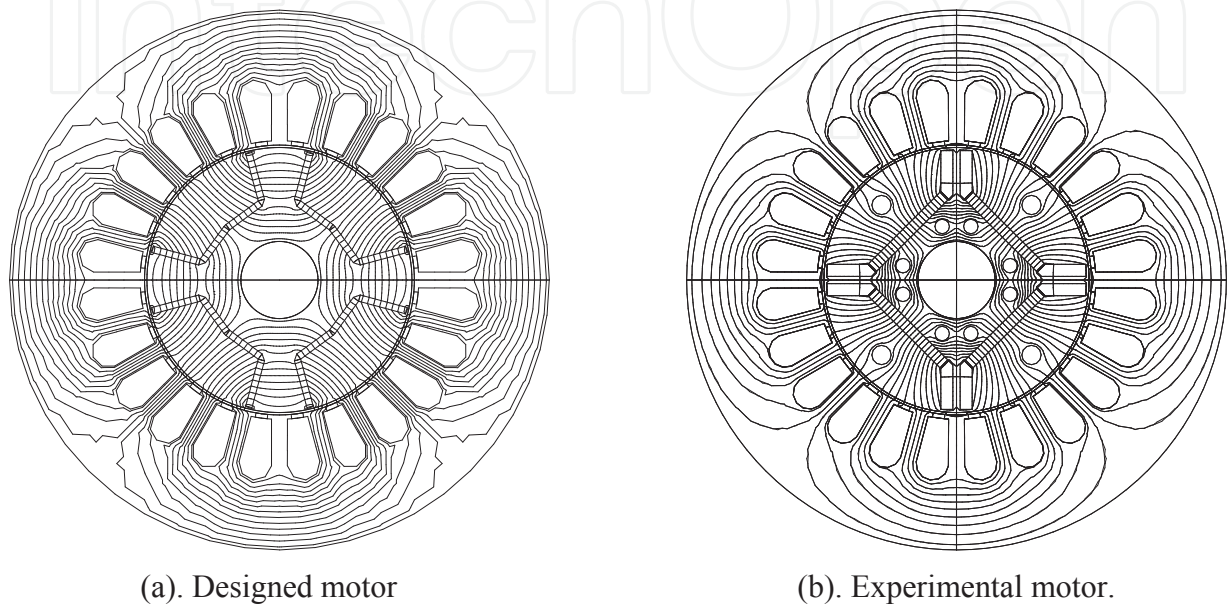


Figure 14. Obtained rotor structure and flux distribution at no load.

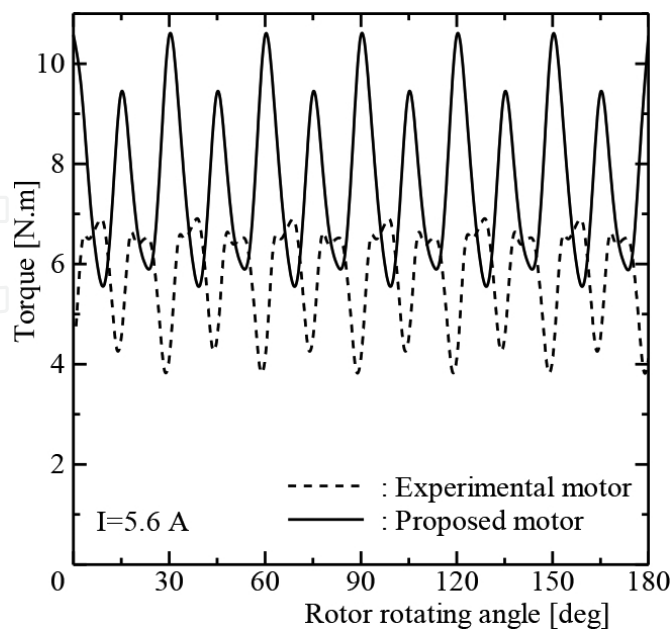


Figure 15. Comparison of torque with the experimental motor.

5. Comparison of measured results

We have manufactured the designed rotor shown in **Figure 14a**. **Figure 16** shows the measured electromotive force when the rotor is rotating at a speed of 1500 min^{-1} . The effective value and fundamental component of the electromotive force are 96.3 and 133.8 V, respectively, and those for the experimental motor are 68.2 and 95.6 V, respectively. Therefore, the electromotive force of the designed motor is 1.4 times larger than that of the experimental motor. **Figure 17** shows the inductance measured by an LCR meter at 100 Hz. The obtained d and q inductances are 12.69 and 28.37 mH, respectively, for the designed motor, and 12.51 and 29.37 mH, respectively, for the experimental motor. The developed torque of IPMSM can be expressed by

$$T = p\Phi I \cos \beta + 0.5p(L_q - L_d)I^2 \sin 2\beta \quad (1)$$

where p , Φ , I , and β are pole pairs, flux linkage, stator current, and phase angle of stator current, respectively. Although $(L_q - L_d)$ of the designed motor is somewhat small, the flux linkage is 1.4 times greater than that of the experimental motor.

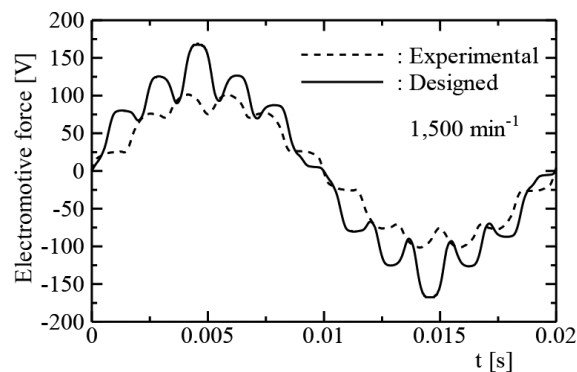


Figure 16. Measured electromotive force.

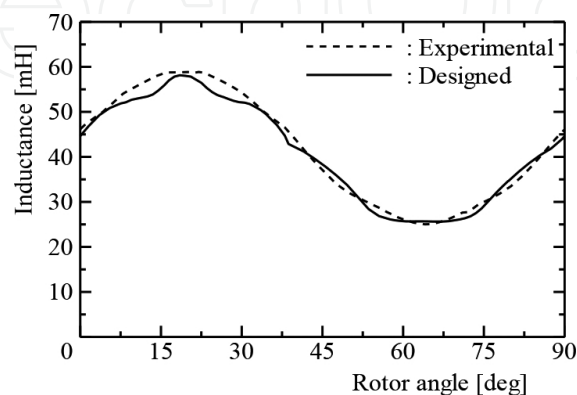


Figure 17. Measured inductance.

Figure 18 shows the torque–current characteristics when β is set to approximately 0. The developed torque calculated by the measured electromotive force is $T = 0.75I$ for the experimental motor and $T = 1.05I$ for the designed motor. These values are approximately the same as the slope shown in **Figure 18**. The differences are generated by the fact that β is not controlled to be exactly 0. Therefore, it is verified that the measured torque of the designed motor is larger than that of the experimental motor under the same stator current.

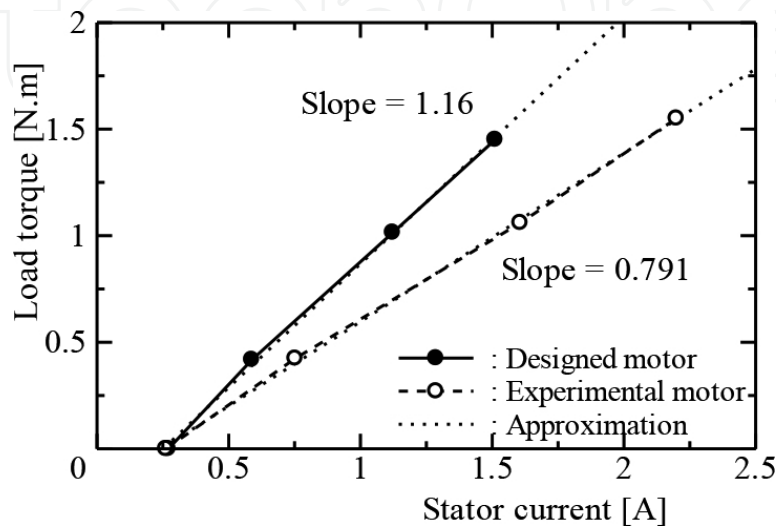


Figure 18. Measured torque characteristics.

6. Conclusions

In this study, we designed the rotor structure of PM synchronous motors. The proposed optimization process combines the topology optimization method and a method that considers the ease of manufacturing. We assumed four hexahedron PMs similar to the rotor shapes obtained by the proposed method for reasons of manufacturing ease. The obtained rotor of the compressor motor for the air-conditioner has 32% more average torque than that of the experimental motor with the same stator. Therefore, the effectiveness of the proposed method is verified.

Author details

Takeo Ishikawa

Address all correspondence to: ishi@gunma-u.ac.jp

Division of Electronics and Informatics, Faculty of Science and Technology, Gunma University, Maebashi, Japan

References

- [1] Z. Q. Zhu, D. Howe, and Z. P. Xia, "Prediction of open-circuit air gap field distribution in brushless machines having an inset permanent magnet rotor topology," *IEEE Trans. Magn.*, vol.30, no.1, pp.98–107, (1994)
- [2] D. N. Dyck and D. A. Lowther, "Automated design of magnetic devices by optimizing material distribution," *IEEE Trans. Magn.*, vol.32, no.3, pp.1188–1193, (1996)
- [3] J. K. Byun, S. Y. Hahn, and I. H. Park, "Topology optimization of electrical devices using mutual energy and sensitivity," *IEEE Trans. Magn.*, vol.35, no.5, pp.3718–3720, (1999)
- [4] C. H. Im, H. K. Jun, and Y. J. Kim, "Hybrid genetic algorithm for electromagnetic topology optimization," *IEEE Trans. Magn.*, vol.39, no.5, pp.2163–2169, (2003)
- [5] S. Wang, D. Youn, H. Moon, and J. Kang, "Topology optimization of electromagnetic systems considering magnetization direction," *IEEE Trans. Magn.*, vol.41, no.5, pp. 1808–1811, (2005)
- [6] H. Shim, S. Wang, and K. Hameyer, "Topology optimization of magneto thermal systems considering eddy current as Joule heat," *IEEE Trans. Magn.*, vol.43, no.4, pp. 1617–1620, (2007)
- [7] D. H. Kim, J. K. Sykulski, and D. A. Lowther, "The implications of the use of composite material in electromagnetic device topology and shape optimization," *IEEE Trans. Magn.*, vol.45, no.3, pp.1154–1157, (2009)
- [8] J. S. Choi and J. Yoo, "Structural topology optimization of magnetic actuators using Genetic algorithms and ON/OFF sensitivity," *IEEE Trans. Magn.*, vol.45, no.5, pp.2276–2279, (2009)
- [9] T. Labbe and B. Dehez, "Convexity-oriented mapping method for the topology optimization of electromagnetic devices composed of iron and coils," *IEEE Trans. Magn.*, vol.46, no.5, pp.1177–1185, (2010)
- [10] J. Lee and N. Kikuchi, "Structural topology optimization of electrical machinery to maximize stiffness with body force distribution," *IEEE Trans. Magn.*, vol.46, no.10, pp. 3790–3794, (2010)
- [11] N. Takahashi, T. Yamada, and D. Miyagi, "Examination of optimal design of IPM motor using ON/OFF method," *IEEE Trans. Magn.*, vol.46, no.8, pp.3149–3152, (2010)
- [12] S. Park and S. Min, "Design of magnetic actuator with nonlinear ferromagnetic material using level-set based topology optimization," *IEEE Trans. Magn.*, vol.46, no.2, pp.618–621, (2010)
- [13] K. Watanabe, F. Campelo, Y. Iijima, K. Kawano, T. Matsuo, T. Mifune, and H. Igarashi, "Optimization of inductors using evolutionary algorithms and its experimental validation," *IEEE Trans. Magn.*, vol.46, no.8, pp.3393–3396, (2010)

- [14] Y. Okamoto, Y. Tominaga, S. Sato, "Topological design for 3-D optimization using the combination of multistep genetic algorithm with design space reduction and nonconforming mesh connection," *IEEE Trans. Magn.*, vol.48, no.2, pp.515–518, (2012)
- [15] Hahn, I., "Heuristic structural optimization of the permanent magnets used in a surface mounted permanent-magnet synchronous machine," *IEEE Trans. Magn.*, vol.48, no.1, pp.118–127, (2012)
- [16] T. Ishikawa, M. Kaneda, and A. Yamagiwa, "Optimal material distribution design of interior permanent magnet synchronous motor using Genetic algorithm," *The 10th biennial IEEE Conference on Electromagnetic Field Computation, Perugia, Italy*, pp. 2–4, (2002)
- [17] T. Ishikawa, K. Yonetake, and N. Kurita, "An optimal material distribution design of brushless DC motor by genetic algorithm considering a cluster of material," *IEEE Trans. Magn.*, vol.47, no.5, pp. 1310–1313, (2011)
- [18] T. Ishikawa and K. Nakayama, "Topology optimization of rotor structure in brushless DC motor with concentrated windings using genetic algorithm combined with cluster of material," *IEEE Trans. Magn.*, vol.48, no.2, pp.899–902, (2012)
- [19] T. Ishikawa, K. Nakayama, N. Kurita, and F. P. Dawson, "Optimization of rotor topology in PM synchronous motors by Genetic algorithm considering cluster of materials and cleaning procedure," *IEEE Trans. on Magnetics*, vol. 50, no. 2, paper no. 7015704, (2014)

